ELSEVIER

Applied Catalysis A: General 197 (2000) 11–21

APPLIED CATALYSIS A: GENERAL

www.elsevier.com/locate/apcata

Simultaneous deactivation by coke and sulfur of bimetallic Pt–Re(Ge, Sn)/Al_2O_3 catalysts for *n*-hexane reforming

A. Borgna, T.F. Garetto, C.R. Apesteguía *

Instituto de Investigaciones en Catálisis y Petroquímica (INCAPE), (UNL-CONICET) Santiago del Estero 2654, 3000 Santa Fe, Argentina

Abstract

The simultaneous deactivation by coke and sulfur of monometallic Pt/Al_2O_3 and bimetallic Pt–Re(Ge, Sn)/Al_2O_3 catalysts was studied using *n*-hexane reforming as bifunctional test reaction and thiophene as poisoning molecule. The residual activities in the activity decay curves were used for measuring the catalyst sensitivity to coke formation and sulfur poisoning. Sulfur and carbonaceous deposits accumulated essentially on the metallic fraction and affected the catalyst activity for both monofunctional metallic and bifunctional metal–acid catalyzed reactions. The overall deactivation rate for *n*-hexane conversion increased in the order Pt–Ge<Pt≪Pt–Sn≤Pt–Re. This deactivation trend resulted from the combination of the catalyst resistance to each individual deactivation process. Pt–Ge/Al_2O_3 was the most stable catalyst essentially because of its high thiotolerance for *n*-hexane transformation reactions and also because it showed low activity for dehydrogenation reactions leading to the formation of coke precursors. Sulfur poisoning on Pt/Al_2O_3 decreased monofunctional metal-catalyzed reactions but concomitantly increased the activity for acid-controlled skeletal rearrangement reactions; as a result, *n*-hexane conversion was only slightly diminished by the addition of sulfur. Pt–Sn/Al_2O_3 showed high resistance to coke deactivation but was severely poisoned by the addition of sulfur. The Pt–Re/Al_2O_3 activity was significantly decreased by both deactivation processes. Changes in catalyst selectivity are interpreted in terms of selective deactivation by coke and sulfur of individual reaction pathways involved in the *n*-hexane reforming mechanism.

Keywords: Simultaneous deactivation; Catalyst thiotolerance; *n*-Hexane reforming; Pt–Re(Ge, Sn)/Al_2O_3 catalysts

1. Introduction

In commercial practice, the catalyst activity decay is often caused by two or more different and concomitant deactivation processes. However, very few papers have been published on catalyst deactivation by simultaneous deactivation processes [1–4], probably because the occurrence of two different deactivation mechanisms complicates both the analysis of experimental results and the measurement of kinetic parameters.

In particular, sulfur poisoning of platinum-based naphtha reforming catalysts takes place under industrial conditions in the presence of simultaneous deactivation by coking. The coadsorption of carbonaceous deposits on platinum may change both the sulfur poisoning and the thermodynamics of sulfur adsorption [5,6]. In previous work [4,7], we have undertaken fundamental studies regarding sulfur poisoning of naphtha reforming catalysts in the presence of coking. Specifically, we employed two monofunctional metallic reactions, benzene (Bz) hydrogenation and cyclopentane hydrogenolysis, to ascertain the effect of sulfur poisoning of monometallic Pt/Al_2O_3 and bimetallic Pt–Re(Ir)/Al_2O_3 catalysts in the presence of

* Corresponding author. Tel.: +54-342-4555279; fax: +54-342-4531068.
E-mail address: capesteg@fiqus.unl.edu.ar (C.R. Apesteguía)

0926-860X/00/$ – see front matter
PII: S0926-860X(99)00528-1

simultaneous coke deactivation. Bz hydrogenation and cyclopentane hydrogenolysis are structure-insensitive and structure-sensitive reactions, respectively, on platinum [8,9]. By employing different approaches for calculating the catalyst thiotolerance in the presence of simultaneous coke deactivation, we established the relative sulfur sensitivities of the catalysts investigated. Nevertheless, main reactions in naphtha reforming are dehydrocyclization and isomerization which proceed via bifunctional mechanisms involving both metallic and acid sites. The catalyst thiotolerance established by using monofunctional metallic reactions does not necessarily reflect the sulfur resistance for bifunctional metal–acid reactions. Thus, in this work, we have extended our previous studies by employing a typical bifunctional reaction in naphtha reforming process, the reforming of *n*-hexane, for studying the simultaneous (C+S) deactivation of Pt–Re(Ge, Sn)/Al_2O_3 catalysts.

2. Experimental

Monometallic Pt catalyst was made by impregnation at 303 K of a high-purity γ-Al_2O_3 powder (Cyanamid Ketjen CK300) with an aqueous solution of chloroplatinic acid and HCl. The CK300 alumina has a BET surface area of 180 $m^2\,g^{-1}$, a pore volume of 0.49 $cm^3\,g^{-1}$ and contains 50 ppm sulfur. After impregnation, the sample was dried 12 h at 393 K and heated in air to 773 K. Next, the chlorine content was regulated using a gaseous mixture of HCl, water and air. Finally, the sample was purged with N_2 and reduced in flowing H_2 for 4 h at 773 K. Bimetallic Pt–Sn catalyst was prepared by coimpregnation of alumina CK300 with an aqueous solution of $Cl_2Sn{\cdot}2H_2O$, H_2PtCl_6 and HCl. Coimpregnation was carried out at 303 K and the volume of the impregnating solution was 0.7 ml g^{-1} support. After drying overnight at 393 K, the sample was calcined in air for 5 h at 773 K, purged in N_2 and reduced in flowing H_2 at the same temperature for 4 h. Bimetallic Pt–Ge catalyst was obtained by employing a similar preparation method. The support was impregnated with a solution containing H_2PtCl_6, $GeCl_4$, and HCl. After successively drying overnight at 393 K and calcining in air for 5 h at 773 K, the sample was reduced in H_2 for 4 h at 773 K. Pt–Re/Al_2O_3 (Cyanamid Ketjen CK433) catalyst was obtained in extrudates from commercial sources and it contains 60 ppm sulfur. The CK433 catalyst extrudates were crushed and the 0.35–0.42 mm fraction fraction was separed and reduced in H_2 at 773 K for 4 h. Metal loadings and the chloride level on the catalysts are given in Table 1. Metal loadings were measured by atomic absorption spectrometry, whereas chlorine contents on the catalysts were determined by chemical analysis, using conventional colorimetric techniques.

Accessible metal fractions were determined by chemisorption of hydrogen, (HC), and oxygen, (OC). The volumetric adsorption experiments were performed at room temperature in a conventional vacuum apparatus. Hydrogen uptake was determined using the double isotherm method [10]: the first isotherm gave the total gas uptake and the second, obtained after 1 h of evacuation at room temperature, the weakly adsorbed gas. By difference, the amount of strongly adsorbed gas was determined. In the case of (OC), a single isotherm was performed for determining (OC) values since the amount of reversible oxygen at room temperature was negligible. The pressure range was

Table 1
Main characteristics of the catalysts used in this work[a]

Catalyst	Metal loading (wt.%)	Cl (wt.%)	Accessible metal fraction (%)	
			(OC)	(HC)
Pt	0.40 Pt	0.95	56	58
Pt–Re	0.31 Pt–0.30 Re	0.78	51[b]	19[c]
Pt–Ge	0.35 Pt–0.24 Ge	0.81	46[c]	12[c]
Pt–Sn	0.28 Pt–0.30 Sn	0.90	51[c]	36[c]

[a] All the catalysts were supported on alumina.
[b] Value calculated by considering the total metal loading.
[c] Values calculated by considering only the Pt loading.

0–7 kPa and extrapolation to zero pressure was used as a measure of the gas uptake on the metal. Samples were reduced in H_2 at 773 K for 2 h prior to performing gas chemisorption experiments.

Catalytic tests were carried out at in a differential fixed-bed reactor at 693 K and 101.3 kPa. *n*-Hexane (Merck, ACS, 99.8% purity) was introduced via syringe pump and vaporized into flowing H_2 to give a H_2/C_6H_{14} molar ratio of 7.8. Hydrogen was passed through Deoxo and molecular sieve drying units. The catalyst bed temperature was controlled to within 1 K. Catalyst loadings of 200 mg, sieved at 0.35–0.42 mm, were used. Prior to catalytic tests, the samples were treated in N_2 at 353 K for 1 h to remove water and then reduced with flowing H_2 for 4 h at 773 K. Catalytic tests were conducted at a weight hourly space velocity (WHSV) of 5.4 h^{-1}. Sulfur poisoning experiments were performed by doping the feed with thiophene in concentrations between 0 and 25 ppm of S. Initial tests repeated six times with the Pt/Al_2O_3 catalyst led to an estimated accuracy of ±4% in the activity measurements. The data reported in the present paper are average values of two repeated runs. The concentrations of unreacted *n*-hexane (*n*-C_6) and of reaction products in the reactor effluent were measured by gas chromatography using a Hewlett–Packard 5890 chromatograph equipped with a flame ionization detector. The following nomenclature was used for identifying the reaction products: gases, G (methane, ethane, propane, *n*-butane and i-butane), paraffins with five carbon atoms, C_5 (*n*-pentane, i-pentane), *n*-hexane isomers, i-C_6 (2-methyl pentane, 3-methyl pentane, 2,2-dimethyl butane, 2,3-dimethyl butane), methylcyclopentane (MCP), and Bz. Traces of cyclopentane, cyclohexane and paraffins with seven carbon atoms were also detected.

3. Results

3.1. Catalyst characterization

Table 1 shows the accessible metal fractions of the catalysts calculated by (HC) and (OC). The values were obtained using stoichiometries of $H/Pt_s=1$ and $O/Pt_s=O/Re_s=1$ and by assuming that the uptakes of both gases on Ge and Sn as well as that of hydrogen on Re were negligible [11,12]. Pt_s and Re_s imply Pt and Re atoms on the surface, respectively. The metallic dispersions of the five samples calculated by (OC) were similar, close to 50%. However, the metallic dispersions of bimetallic catalysts calculated by (HC) were significantly lower than those obtained through (OC). The low values measured for (HC) on bimetallic catalysts probably reflect the formation of bimetallic clusters or alloys caused by the previous catalyst reduction in H_2 at 773 K. The diminution of hydrogen uptake on bimetallic Pt–X catalysts, where X is a second metal, that does not chemisorb H_2, has been rationalized in terms of a geometric effect: (HC) decreases because Pt is 'diluted' by the X atoms which reduce the number of Pt ensembles needed to adsorb H_2 dissociatively [13].

3.2. Catalytic tests: deactivation by coke formation

Fig. 1 illustrates the time-on-stream behavior of the catalysts during sulfur-free *n*-hexane reforming reactions. Over all the catalysts, the *n*-C_6 conversion (X) diminished with time because of coke formation. Qualitatively, similar deactivation curves were obtained when X_i, the conversion to product i, was represented as a function of time-on-stream. By extrapolating the deactivation curves to 0, we determined

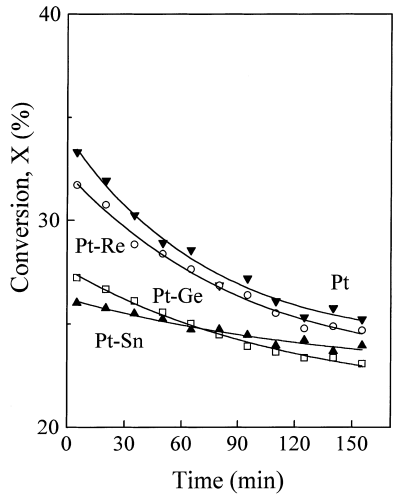

Fig. 1. Time dependence of *n*-hexane conversion for sulfur-free *n*-hexane reforming on Pt/Al_2O_3 and Pt–Re(Ge, Sn)/Al_2O_3 catalysts (T=693 K, P=101.3 kPa, H_2/*n*-hexane=7.8, WHSV=5.4 h^{-1}).

Table 2
Initial reaction rates for sulfur-free *n*-hexane reforming on Pt and Pt–Re(Ge, Sn) catalysts[a]

Catalyst	r_0[b]	r_G^0[c]	$r_{C_5}^0$[c]	$r_{i\text{-}C_6}^0$[c]	r_{MCP}^0[c]	r_{Bz}^0[c]
Pt	22.8	1.74	0.84	13.0	3.75	3.62
Pt–Re	21.9	1.81	0.78	12.1	3.30	2.65
Pt–Ge	18.2	0.58	0.06	15.8	1.33	0.65
Pt–Sn	17.3	0.52	0.06	14.4	1.33	0.58

[a] T=693 K, P=101.3 kPa, H_2/*n*-hexane=7.8, WHSV=5.4 h^{-1}.
[b] Reaction rate for *n*-hexane conversion at zero time (mmol *n*-hexane/h g catalyst).
[c] Reaction rate for the formation of product *i* at zero time (mmol product *i*/h g catalyst).

the values of X_0 and X_i^0, and calculated the initial rate for *n*-hexane conversion (r_0) and for the formation of product *i* (r_i^0). Results are shown in Table 2. Pt/Al_2O_3 and $Pt–Re/Al_2O_3$ were more active for converting *n*-hexane than $Pt–Ge(Sn)/Al_2O_3$ catalysts. In all the cases, i-C_6 isomers were the predominant products of the reaction, but $r_{i\text{-}C_6}^0$ values were higher on Pt–Ge(Sn) than on Pt and Pt–Re catalysts. The highest formation rate of Bz was measured on monometallic Pt/Al_2O_3, whereas bimetallic $Pt–Re/Al_2O_3$ was particularly active for producing gases. The formation rates of Bz and C_5 were significantly lower on $Pt–Ge(Sn)/Al_2O_3$ than on Pt and Pt–Re catalysts.

The catalyst deactivation caused by formation of coke was studied from the curves representing the activity decay as a function of time (Fig. 2). The activity for sulfur-free *n*-hexane reforming is defined as $a^C = r_t^C/r_0$, where r_t^C is the *n*-hexane conversion rate without sulfur poisoning at time *t*. Similarly, the activity for the formation of the product *i* is defined as $a_i^C = r_{it}^C/r_{i0}$. Fig. 2 shows that *n*-C6 conversion was less inhibited by coking on $Pt–Sn(Ge)/Al_2O_3$ than on Pt/Al_2O_3 or $Pt–Re/Al_2O_3$. In the a_i^C versus *t* curves (not shown here), the pseudo-steady-state activities, $a_i^{C,SS}$, measured after 150 min on stream, were taken as deactivation parameters to establish the relative catalyst sensitivity to coke deactivation for the formation of product *i*. The obtained $a_i^{C,SS}$ values are given in Table 3. Column 4 shows that the $a_{i\text{-}C_6}^{C,SS}$ values were between 0.85 and 0.90 for all the catalysts, thereby indicating that isomerization was slightly affected by coke formation. Aromatization was the most deactivated reaction (column 6, $a_{Bz}^{C,SS}$ values).

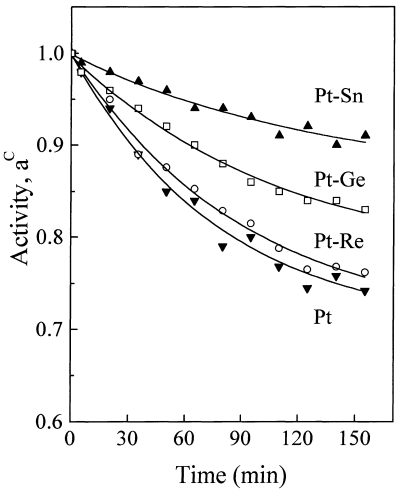

Fig. 2. Deactivation by coking. Time evolution of the activity (a^C) for reforming of *n*-hexane fed without sulfur on Pt/Al_2O_3 and $Pt–Re(Ge, Sn)/Al_2O_3$ catalysts.

3.3. Catalytic tests: simultaneous deactivation by coke and sulfur

Fig. 3 shows the catalyst activity decay curves obtained for the reforming of *n*-hexane fed with 15.5 ppm S. The a^T versus *t* curves reflect the activity decay caused by simultaneous coking and sulfur deactivation. It is observed that Pt/Al_2O_3 and $Pt–Ge/Al_2O_3$ were significantly more resistant to (C+S) deactivation than Pt–Sn and Pt–Re catalysts.

The activity decay caused by sulfur alone can not be determined directly from our experimental data, but the sulfur poisoning curves may be obtained by assuming that sulfur and coke deactivation rates are additives. This hypothesis of independence of simultaneous deactivation processes implies that the overall

Table 3
Deactivation by coking for sulfur-free *n*-hexane reforming[a]

Catalyst	$a_G^{C,SS}$	$a_{C_5}^{C,SS}$	$a_{i\text{-}C_6}^{C,SS}$	$a_{MCP}^{C,SS}$	$a_{Bz}^{C,SS}$
Pt	0.70	0.62	0.87	0.73	0.51
Pt–Re	0.60	0.58	0.90	0.71	0.54
Pt–Ge	0.76	0.73	0.87	0.89	0.67
Pt–Sn	0.92	0.91	0.90	0.95	0.82

[a] Residual activities for the formation of product *i* ($a_i^{C,SS}$) measured after 150 min on stream; T=693 K, P=101.3 kPa, H_2/*n*-hexane=7.8, WHSV=5.4 h^{-1}.

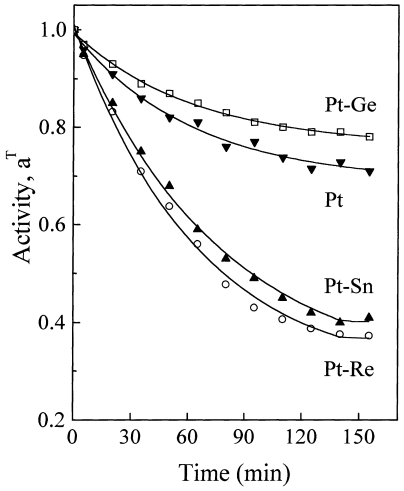

Fig. 3. Simultaneous deactivation by coke and sulfur. Time evolution of the activity (a^T) for reforming of *n*-hexane fed with 15.5 ppm S on Pt/Al_2O_3 and Pt–Re(Ge, Sn)/Al_2O_3 catalysts.

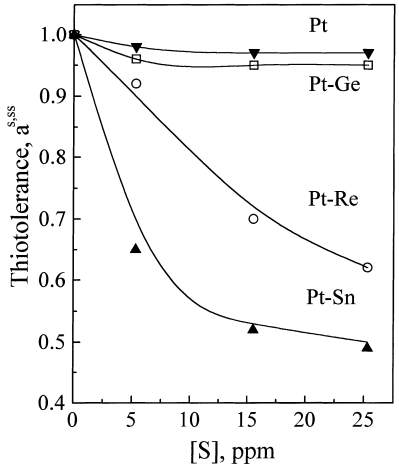

Fig. 5. Catalyst thiotolerance ($a^{S,SS}$) for *n*-hexane conversion as a function of sulfur concentration over Pt/Al_2O_3 and Pt–Re(Ge, Sn)/Al_2O_3 catalysts.

deactivation rate is a simple sum of each individual deactivation rate. The activity decay caused by sulfur alone (a^S) can then be calculated from a^T and a^C decay curves as $a^S=1+a^T-a^C$. Fig. 4 illustrates the values of a^S obtained from a^C versus t (deactivation by coking) and a^T versus t (overall deactivation by coke and sulfur) curves on Pt–Re/Al_2O_3 catalyst for 25.2 ppm S.

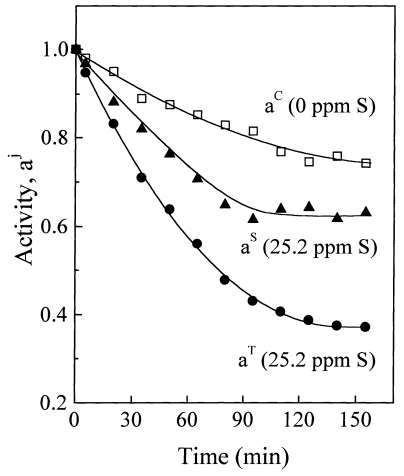

Fig. 4. Activity decay curves representing coking deactivation (a^C), sulfur deactivation (a^S), and overall (C+S) deactivation (a^T) for *n*-hexane conversion on Pt–Re/Al_2O_3. The a^S vs. t curve is obtained from a^T vs. t and a^C vs. t curves as $a^S=1+a^T-a^C$.

Thiotolerance ($a^{S,SS}$), which is defined as the pseudo-steady-state activity in the sulfur deactivation curves, was used for determining the relative catalyst sensitivity to sulfur poisoning. The catalyst thiotolerance for *n*-hexane conversion was calculated as $a^{S,SS}=1+a^{T,SS}-a^{C,SS}$, where $a^{C,SS}$ and $a^{T,SS}$ are the residual activities in the activity decay caused by coking alone and by (C+S) deactivation, respectively. Similarly, the catalyst thiotolerance for the formation of product i was calculated as $a_i^{S,SS} = 1 + a_i^{T,SS} - a_i^{C,SS}$. All the pseudo-steady-state activities were measured in the activity decay curves after 150 min on stream. The thiotolerance of Pt and Pt–Re(Ge, Sn) catalysts for *n*-hexane conversion is represented in Fig. 5 as a function of the sulfur concentration in the feed, whereas in Table 4 are shown

Table 4
Reforming of *n*-hexane fed with 15.5 ppm S on Pt and Pt–Re(Ge, Sn) catalysts[a]

Catalyst	$a_G^{S,SS}$	$a_{C_5}^{S,SS}$	$a_{i\text{-}C_6}^{S,SS}$	$a_{MCP}^{S,SS}$	$a_{Bz}^{S,SS}$
Pt	0.74	0.52	1.13	0.83	0.77
Pt–Re	0.63	0.47	0.64	0.67	0.56
Pt–Ge	0.94	0.71	0.90	0.98	0.90
Pt–Sn	0.53	0.44	0.62	0.86	0.53

[a] Catalyst thiotolerance for the formation of product i ($a_i^{S,SS}$); T=693 K, P=101.3 kPa, H_2/*n*-hexane=7.8, WHSV=5.4 h^{-1}.

Table 5
Reforming of *n*-hexane fed with 15.5 ppm S on Pt and Pt–Re(Ge, Sn) catalysts[a]

Catalyst	$\Phi_G^{S,SS}$	$\Phi_{C_5}^{S,SS}$	$\Phi_{i\text{-}C_6}^{S,SS}$	$\Phi_{MCP}^{S,SS}$	$\Phi_{Bz}^{S,E}$
Pt	0.60	0.38	1.28	0.75	0.56
Pt–Re	0.77	0.50	1.11	0.86	0.46
Pt–Ge	1.00	1.00	0.91	1.48	0.86
Pt–Sn	1.00	1.00	0.81	1.66	0.69

[a] Residual normalized selectivities to product i ($\Phi_i^{S,SS}$) obtained from sulfur poisoning curves; T=693 K, P=101.3 kPa, H_2/*n*-hexane=7.8, WHSV=5.4 h^{-1}.

the $a_i^{S,SS}$ values obtained when the reactant was doped with 15.5 ppm S. From Fig. 5, it is inferred that the catalyst thiotolerance for *n*-C_6 conversion follows the order Pt≅Pt–Ge≫Pt–Re>Pt–Sn. On the other hand, Table 4 shows that the $a_{C_5}^{S,SS}$, $a_{Bz}^{S,SS}$ and $a_G^{S,SS}$ values decrease in the order Pt–Ge>Pt>Pt–Re>Pt–Sn, whereas in the case of $a_{i\text{-}C_6}^{S,SS}$, the trend is Pt>Pt–Ge>Pt–Re≅ Pt–Sn.

The effect of sulfur poisoning on catalyst selectivity was studied by determining the steady-states values in the curves representing the normalized selectivity as a function of time. The normalized selectivity to product i (Φ_i) is defined as $\Phi_i = S_{it}/S_{i0}$ where S_{i0} and S_{it} are the selectivities to product i at time zero and time t, respectively. In a manner similar to the case of thiotolerance, the residual normalized selectivity in the sulfur poisoning curves is calculated as $\Phi_i^{S,SS} = 1 + \Phi_i^{T,SS} - \Phi_i^{C,SS}$, where $\Phi_i^{C,SS}$ and $\Phi_i^{T,SS}$ are the residual normalized selectivities in the selectivity decay caused by coking alone and by (C+S) deactivation, respectively. The $\Phi_i^{S,SS}$ values obtained for 15.5 ppm S are summarized in Table 5. It is observed that sulfur poisoning clearly changes the selectivity of fresh Pt and Pt–Re catalysts by increasing the isomerization selectivity at the expense of the other reactions. On Pt–Ge(Sn) catalysts, the $\Phi_G^{S,SS}$ and $\Phi_{C_5}^{S,SS}$ values were practically not modified by sulfur poisoning, but the normalized selectivity to MCP was clearly increased. The different qualitative selectivity changes induced by sulfur addition on Pt–Ge(Sn)/Al_2O_3 as compared to Pt and Pt–Re catalysts are shown in Figs. 6 and 7 where the $\Phi_{i\text{-}C_6}^{S,SS}$ and $\Phi_{MCP}^{S,SS}$ values are, respectively, plotted as a function of the sulfur concentration in the feed.

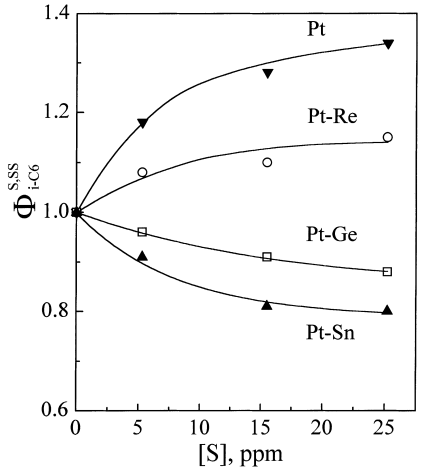

Fig. 6. Residual normalized selectivity to i-C_6 isomers ($\Phi_{i\text{-}C_6}^{S,SS}$) as a function of the sulfur concentration in the feed over Pt/Al_2O_3 and Pt–Re(Ge, Sn)/Al_2O_3 catalysts.

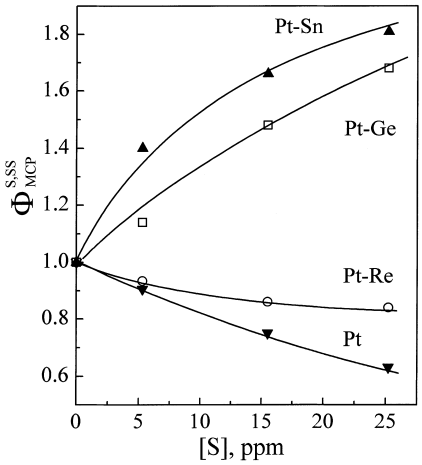

Fig. 7. Residual normalized selectivity to MCP ($\Phi_{MCP}^{S,SS}$) as a function of the sulfur concentration in the feed over Pt/Al_2O_3 and Pt–Re(Ge, Sn)/Al_2O_3 catalysts.

4. Discussion

The catalytic reforming of naphtha requires bifunctional catalysts for increasing the aromatic contents of naphthas, and consequently, their octane number. The transformation of *n*-hexane is a typical naphtha reforming reaction and several authors have studied the bifunctional mechanism for *n*-hexane reforming on monometallic Pt [14–16] and bimetallic Pt–Re(Sn,

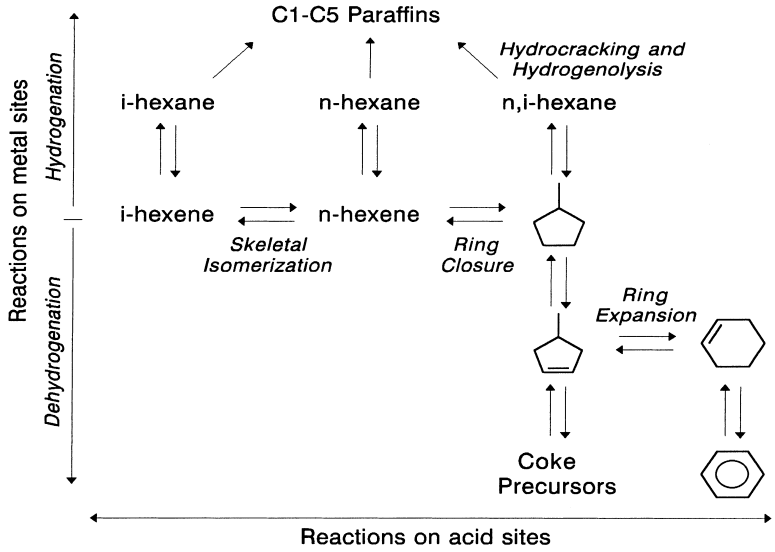

Fig. 8. Simplified reaction network for *n*-hexane reforming reactions.

Ge) [17–19] catalysts. Based on this bibliography, we present in Fig. 8 a simplified scheme of the reaction network for *n*-hexane reforming. The reaction network includes: (a) the isomerization and the dehydrocyclization of *n*-C_6 to i-C_6 and MCP, respectively, through bifunctional mechanisms involving metal- and acid-catalyzed steps; (b) the hydrogenolysis and hydrocracking of *n*-C_6 and i-C_6 to C_1–C_5 paraffins; (c) the aromatization of MCP to Bz through the ring expansion reaction of methylcyclopentene (MCPe); (d) dehydrogenation of MCPe to methylcyclopentadiene (MCPde) producing coke precursors.

Table 2 shows the initial rate values for *n*-C_6 conversion (r_0) and for the formation of product *i* (r_i^0) obtained on different naphtha reforming catalysts. In all the cases, isomerization to i-C_6 was the preferential pathway for *n*-hexane conversion reactions, but $r^0_{\text{i-C}_6}$ was higher on Pt–Ge(Sn) than on Pt or Pt–Re catalysts. The isomerization of *n*-paraffins may occur over the metallic fraction via a bond shift or a cyclic mechanism [20], but under reforming conditions, formation of i-C_6 isomers from *n*-hexane takes place essentially via a bifunctional metal–acid mechanism involving the *n*-C_6 dehydrogenation on the metal and the subsequent olefin isomerization on acid sites [21,22]. This bifunctional reaction network is controlled by the acid function which in naphtha reforming catalysts essentially depends on the chloride level on the catalyst. Our catalysts contain similar amounts of chlorine (Table 1), between 0.78 and 0.95 wt.%, and this suggests that the higher isomerization activity on Pt–Ge(Sn) catalysts is not related to the acid function but to metallic-catalyzed reactions. The values of $r^0_{C_5}$ in Table 2 show that hydrogenolysis of *n*-C_6 to C_5 paraffins is severely depleted on Pt–Ge(Sn)/Al_2O_3 catalysts, probably because the presence of inactive Ge(Sn) atoms drastically diminishes the number of Pt ensembles required for achieving C–C terminal bond scissions [23,24]. Such an activity decrease for hydrogenolysis of C_6 paraffins increases the abundance of intermediates available for isomerization and may explain the higher isomerization activity measured on Pt–Ge(Sn) catalysts.

Dehydrocyclization of *n*-C_6 to MCP occurs via a bifunctional metal–acid mechanism [22]; *n*-hexane is transformed on metal sites to *n*-hexene which then produces MCP on acid sites. Nevertheless, under low pressure conditions, the *n*-hexane ring closure to MCP may also occur exclusively on metal sites via dienes and trienes intermediates [25]. On the other hand, the MCP ring expansion to Bz is a bifunctional reaction controlled by the acid function [26]. MCP is first dehydrogenated on the metal to MCPe and then transformed on acid sites to cyclohexene which is

immediately dehydrogenated to Bz. Thus, in the reaction network of Fig. 8, MCP is the key intermediate for the reforming of *n*-C_6 to Bz. The amount of MCP detected in the products is the difference between the formation rate of MCP from *n*-C_6 and the transformation rate of MCP to Bz and other products, particularly dehydrogenated MCP species leading to coke precursors. Our results show that both the formation rate of Bz (Table 2) and the hydrogen uptake (Table 1) are significantly lower on Pt–Ge(Sn) catalysts than on monometallic Pt/Al_2O_3. This is consistent with previous studies showing that hydrogenation/dehydrogenation reactions on Pt are severely depressed in Pt–Ge(Sn) catalysts, particularly in low pressure conditions [11,27,28]. The introduction of an inert Ge(Sn) atom enlarged the distance between the two Pt atoms needed for dissociative H_2 adsorption which becomes an activated process [29]; as a result, both the hydrogen coverage and the hydrogenation activity diminish. Regarding the Pt and Pt–Re catalysts, Pt is a better dehydrogenation metal than Re [30] and this explains that r^0_{Bz} is higher on Pt/Al_2O_3 than on Pt–Re/Al_2O_3 (Table 2). On the contrary, the formation rate of C_5 paraffins and lighter hydrocarbons was higher on Pt–Re catalyst because Re is known to promote hydrogenolysis reactions [31].

As concerns coke deactivation, Pt–Ge(Sn)/Al_2O_3 catalysts were less affected by coking than Pt/Al_2O_3 and Pt–Re/Al_2O_3 (Fig. 2). As stated by various authors [32,33], in *n*-C_6 reforming, MCPde is the key intermediate for producing coke via consecutive condensation reactions. The formation of coke precursors is inhibited over Pt–Ge(Sn) catalysts because they display low activity for the transformation of MCPe to MCPde and to the further MCPde dehydrogenation. Pt–Sn/Al_2O_3 was particularly resistant to coke deactivation. This is consistent with the results obtained by Beltramini and Trimm [34] who postulated that the ability to decrease coke formation results from enhanced gasification of coke precursors by tin. Others authors have suggested that tin inhibits coke formation by forming ensembles with platinum that do not favor the production of carbonaceous deposits [35]. In contrast to coking on Pt–Sn/Al_2O_3, the activity for *n*-hexane conversion on monometallic Pt catalyst was significantly decreased by coke formation. Pt/Al_2O_3 is highly active for dehydrogenation reactions and shows the highest formation rate of Bz (Table 2). In the reaction network of Fig. 8, Pt/Al_2O_3 promotes deeper dehydrogenation pathways, therefore producing more coke and Bz.

In all the cases, *n*-C_6 isomerization to i-C_6 was only slightly affected by coking (Table 3, column 4). Several studies on coke formation over metal supported catalysts agree in that coke precursors are initially formed on the metal surface, and then, through a slow diffusion mechanism, are condensed and accumulated on the support [36]. Thus, we can expect that, in our short-term catalytic tests, the formation of coke deactivates essentially the metallic function. This interpretation explains why the acid-controlled formation of i-C_6 isomers is practically not deactivated by coking. The assumption that coke forms predominantly on the metal sites is strengthened by the fact that monofunctional metal-catalyzed pathways leading to the formation of C_5 and Bz were preferentially deactivated by coking.

Thiotolerance was calculated by assuming the hypothesis of independent deactivations (Fig. 4) and was used as deactivation parameter for establishing the catalyst sensitivity to sulfur poisoning. The catalyst thiotolerance for the *n*-hexane conversion followed the order Pt≅Pt–Ge≫Pt–Re>Pt–Sn (Fig. 5). However, the thiotolerance trend is different when the individual reactions involved in *n*-hexane reforming mechanism are analyzed separately. In fact, the $a^{S,SS}_{C_5}$, $a^{S,SS}_{Bz}$ and $a^{S,SS}_{G}$ values followed the order Pt–Ge>Pt>Pt–Re>Pt–Sn, whereas in the case of $a^{S,SS}_{i\text{-}C_6}$, the trend was Pt>Pt–Ge>Pt–Re≅Pt–Sn (Table 4). These results may be explained by considering the nature of the sulfur adsorption on the catalysts. The adsorption of sulfur on Pt-based supported catalysts takes place on both the metal and the support [37–39]. Part of the adsorbed sulfur is resistant to H_2 treatment at 773 K (S_i, irreversibly held sulfur) and is located on the metal. The other part of the adsorbed sulfur is eliminated in H_2 at 773 K and is probably located on both metal and support sites. When the partial pressure of the sulfur compound in the gas phase is low (as in the present work), only the irreversible sulfur on the metal is retained by the catalyst. Thus, the catalyst thiotolerance for a metallic reaction is related to the irreversibly held sulfur on the catalyst: the lower the S_i amount, the higher the thiotolerance [40]. With the exception of the Pt–Sn catalyst, the catalyst thiotolerance trend determined here for the metal-controlled

formation of Bz, C_5 and gases was similar to that found for cyclohexane dehydrogenation, a monofunctional metallic reaction on Pt [40]. The Pt–Ge catalyst exhibited the highest values of $a_{C_5}^{S,SS}$, $a_{Bz}^{S,SS}$, $a_{MCP}^{S,SS}$ and $a_{G}^{S,SS}$. This superior performance is attributed to the formation of Pt–Ge clusters upon H_2 reduction at 773 K that decreases the electronic density of platinum, thereby weakening the strength of the sulfur–platinum bond [41]. Germanium inhibits the adsorption of irreversible sulfur on Pt, and as a result, the Pt thiotolerance in the Pt–Ge/Al_2O_3 catalyst increases. In the case of Pt–Re/Al_2O_3, the adsorption of sulfur on Re is thermodynamically favored compared to Pt and preferentially forms surface Re sulfide [42]. A number of papers have confirmed that Re adsorbs more sulfur than Pt and that sulfur is more strongly bonded to Re than Pt [43,44]. This is consistent with the low thiotolerance exhibited here by the Pt–Re catalyst for metal-controlled reactions. Pt–Sn/Al_2O_3 showed the lowest thiotolerance for the formation of Bz, C_5 and gases. However, sulfur does not adsorb on tin [40,45] and the amount of S_i on Pt in Pt–Sn/Al_2O_3 is about the same as on monometallic Pt/Al_2O_3. The low thiotolerance displayed by Pt–Sn catalysts can not therefore be explained only by the characteristics of the sulfur adsorption on the metal fraction. Probably, the sensitivity to sulfur poisoning was enhanced because the formation of coke is suppressed over Pt–Sn/Al_2O_3 (Fig. 2). It has been reported that coke formation may protect the metal against sulfur poisoning [46]; this protective effect for sulfur adsorption would be negligible on the Pt–Sn catalyst.

As stated above, the catalyst thiotolerance trend for acid-controlled isomerization of *n*-C_6 to i-C_6 (Table 3, column 4) is different from that observed for metal-controlled reactions. Sulfur practically did not affect the isomerization activity of the Pt–Ge catalyst and this is attributable to the inhibition by Ge of the S adsorption on Pt active sites. i-C_6 formation was similarly inhibited on Pt–Re and Pt–Sn catalysts but for different reasons. Sulfur is strongly bonded to Re and the amount of Si per metal surface atom is higher on Pt–Re/Al_2O_3 than on Pt/Al_2O_3. Thus, the metallic function and the hydrogenation activity are drastically poisoned on Pt–Re catalysts as the sulfur feed concentration is increased. As a consequence, the *n*-C_6 isomerization to i-C_6, which is controlled by the acid sites on fresh Pt–Re catalysts, starts being controlled by the metallic function upon sulfur poisoning because the number of accessible metal sites is drastically depleted. On Pt–Sn/Al_2O_3, the amount of S_i is lower than on Pt–Re/Al_2O_3. However, the fresh Pt–Sn catalyst shows low dehydrogenation activity and the addition of small amounts of sulfur further decreases the *n*-C_6 dehydrogenation rate to *n*-hexene. *n*-Hexane isomerization on Pt–Sn/Al_2O_3 therefore starts being controlled by the metallic function at a lower S coverage as compared to Pt–Re/Al_2O_3. Finally, the isomerization activity on Pt/Al_2O_3 catalyst increased upon the addition of thiophene-doped *n*-hexane. Formation of i-C_6 isomers on Pt/Al_2O_3 continues to be controlled by the acid function, at least up to the feed S concentration used in this work, because the high dehydrogenation activity exhibited by the fresh catalyst compensates the partial blocking of the metal function by sulfur. Sulfur is not adsorbed on the support and we can therefore exclude the possibility that the catalyst acidity will increase upon S addition. Probably, the increase in the isomerization activity on Pt/Al_2O_3 upon sulfur addition is due to an 'indirect control' of the metallic function on i-C_6 production [47]. In fact, by partially poisoning the metallic function, sulfur decreases both the hydrocracking of C_6 paraffins and the transformation of olefins to MCP, thereby increasing the abundance of intermediates available for isomerization.

The effect of sulfur poisoning on MCP formation is difficult to interpret not only because MCP is formed via both monofunctional metallic and bifunctional acid-controlled mechanisms but also because MCP is consecutively transformed to Bz and coke precursors. Sulfur poisoning of metal sites primarily depresses dehydrogenation reactions forming olefins and Bz; however, as in the case of isomerization, the acid-controlled cyclization pathway leading to MCP formation may start being controlled by the metal function upon a drastic diminution of the number of accessible metal sites by poisoning.

Sulfur poisoning changes the selectivity of fresh catalysts for *n*-hexane conversion reactions. Depending on the catalyst, sulfur-induced selectivity changes are qualitatively different. While on Pt/Al_2O_3 and Pt–Re/Al_2O_3 catalysts, the isomerization selectivity is enhanced by sulfur poisoning, on Pt–Ge(Sn) catalysts, the addition of sulfur increases the selectivity to MCP (Figs. 6 and 7). These selectivity changes

reflect the selective sulfur poisoning of individual pathways in the *n*-hexane reforming reaction network, as discussed above.

The activity decay curves of Fig. 3 represent the simultaneous deactivation by coke and sulfur of Pt and Pt–Re(Ge, Sn) catalysts for *n*-hexane conversion and show that the catalyst stability is in the order Pt–Ge>Pt≫Pt–Sn≥Pt–Re. This stability trend may be explained by considering the catalyst resistance to each individual deactivation process. Pt–Ge/Al_2O_3 is the most stable catalyst essentially because of its high thiotolerance for all the *n*-hexane conversion reactions and also because it forms less coke precursors than Pt and Pt–Re catalysts. The Pt/Al_2O_3 activity for *n*-hexane conversion decreases because of coke formation, but it remains practically unaffected by cofeeding sulfur with the reactant. Sulfur poisoning on Pt/Al_2O_3 decreases monofunctional metal-catalyzed reactions but concomitantly increases the catalyst activity for skeletal rearrangement reactions; as a result, *n*-hexane conversion is only slightly diminished by the addition of sulfur. Pt–Sn/Al_2O_3 shows high resistance to coke deactivation, but *n*-hexane conversion declines drastically because the catalyst is severely poisoned by the addition of sulfur. Finally, *n*-hexane conversion on Pt–Re catalyst is severely decreased by both deactivation processes.

5. Conclusions

Conclusions of the present study on the simultaneous deactivation by coke and sulfur of Pt/Al_2O_3 and Pt–Re(Ge, Sn)/Al_2O_3 catalysts for *n*-hexane conversion reactions are summarized as follows:

1. Metal-controlled *n*-hexane conversion reactions such as aromatization and hydrogenolysis are less affected by coking on Pt–Ge(Sn)/Al_2O_3 than on Pt and Pt–Re catalysts. Coke formation is inhibited on Pt–Ge(Sn)/Al_2O_3 because these catalysts present low activity for the production of highly dehydrogenated hydrocarbons which are the intermediate species required for coking. Acid-controlled *n*-hexane conversion reactions such as the formation of i-C_6 isomers are only slightly affected by coking over all the catalysts because, in our short-term catalytic tests, coke precursors are essentially formed on the metallic function.
2. The catalyst thiotolerance for *n*-hexane conversion follows the order Pt≅Pt–Ge≫Pt–Re>Pt–Sn. However, the thiotolerance trend is different for the individual reaction pathways involved in the *n*-hexane reforming mechanism. In fact, while the sulfur tolerance for metal-controlled reactions decreases in the sequence Pt–Ge>Pt>Pt–Re>Pt–Sn, the thiotolerance trend for acid-controlled *n*-hexane isomerization is Pt>Pt–Ge>Pt–Re≅Pt–Sn. The catalyst thiotolerance for monofunctional metallic reactions is essentially related to the sulfur adsorption strength on platinum: the lower the amount of irreversibly held sulfur, the higher the thiotolerance. In the case of *n*-hexane isomerization, the addition of sulfur to the reactant increases the formation rate of i-C_6 isomers on Pt/Al_2O_3 because sulfur selectively poisons the hydrocracking of C_6 paraffins and the transformation of olefins to MCP and thereby increases the abundance of intermediates available for isomerization.
3. The catalyst resistance to the simultaneous deactivation by coke and sulfur for *n*-hexane conversion decreases following the sequence Pt–Ge>Pt≫Pt–Sn≥Pt–Re. This stability trend results from the combination of the catalyst resistance to each individual deactivation process. The overall deactivation rate is lower on Pt–Ge/Al_2O_3 essentially because of its superior thiotolerance for all *n*-hexane conversion reactions. On the contrary, the Pt–Sn catalyst is severely poisoned by the addition of sulfur; thus, the activity for *n*-hexane conversion declines drastically on Pt–Sn/Al_2O_3 in spite of its high resistance to coke deactivation. In the case of Pt–Re catalyst, both the formation of coke and the sulfur poisoning significantly affect the catalyst activity for *n*-hexane conversion.

Acknowledgements

Support of this work by the Consejo Nacional de Investigaciones Científicas y Técnicas (CONICET), Argentina, and the Universidad Nacional del Litoral, Santa Fe, Argentina, is gratefully acknowledged.

References

[1] C. Mirodatos, H. Praliaud, M. Primet, in: Proceedings of the 9th Iberoamerican Symposium on Catalysis, Vol. 1, Lisbon, Portugal, 1984, p. 561.
[2] G.J. Stiegel, R.E. Tischer, D.L. Cillo, N.K. Karain, Ind. Eng. Chem. Prod. Res. Dev. 24 (1985) 206.
[3] J. Corella, A. Monzón, Ind. Eng. Chem. Res. 27 (1988) 369.
[4] C.R. Apesteguía, T.F. Garetto, A. Borgna, in: C.H. Bartholomew, J.B. Butt (Eds.), Catalyst Deactivation 1991, Elsevier, Amsterdam, 1991, p. 399.
[5] C.R. Apesteguía, J. Barbier, Bull. Soc. Chim. France 5/6 (1982) 1.
[6] C.M. Pradier, E. Margot, Y. Berthier, J. Oudar, Appl. Catal. 43 (1988) 177.
[7] T.F. Garetto, A. Borgna, A. Monzón, C.R. Apesteguía, in: Proceedings of the 10th Iberoamerican Symposium on Catalysis, Vol. 2, Segovia, Spain, 1992, p. 1257.
[8] P.C. Aben, J.C. Platteeuw, B. Stouthamer, in: Proceedings of the 4th International Congress on Catalysis, Moscú, 1968, p. 31.
[9] C.R. Apesteguía, N. Martin, P. Marecot, A. Morales, J. Barbier, R. Maurel, in: Proceedings of the 7th Iberoamerican Symposium on Catalysis, La Plata, Argentina, 1980, p. 444.
[10] J.H. Sinfelt, J.L. Carter, D.J.C. Yates, J. Catal. 24 (1972) 283.
[11] J. Goldwasser, B. Arenas, C. Bolívar, G. Castro, A. Rodríguez, A. Fleitas, J. Girón, J. Catal. 100 (1986) 75.
[12] J. Barbier, H. Charcosset, G. Pereira, J. Rivière, Appl. Catal. 1 (1981) 71.
[13] V. Ponec, Adv. Catal. 32 (1983) 149.
[14] G.A. Mills, H. Heinemann, T.H. Milliken, A.G. Oblad, Ind. Eng. Chem. 45 (1953) 134.
[15] E. Santacesaria, D. Gelosa, S. Carra, I. Adami, Ind. Eng. Chem. Prod. Res. Dev. 17 (1978) 68.
[16] G.B. Marin, G.F. Froment, Chem. Eng. Sci. 37 (1982) 759.
[17] D. Selman, A. Voorhies, Ind. Eng. Chem. Prod. Res. Dev. 14 (1975) 12.
[18] J.M. Parera, J.N. Beltramini, C.A. Querini, E.E. Martinelli, E.J. Churin, P.E. Aloe, N.S. Fígoli, J. Catal. 99 (1986) 39.
[19] J. Margitfalvi, S. Göbölös, E. Talas, M. Hegedüs, P. Szedlacsek, in: B. Delmon, G.F. Froment (Eds.), Catalyst Deactivation 1987, Elsevier, Amsterdam, 1987, p. 147.
[20] G. Maire, F. Garin, J. Mol. Catal. 48 (1988) 99.
[21] B.C. Gates, J.R. Katzer, G.C.A. Schuit, Chemistry of Catalytic Processes, McGraw-Hill, New York, 1979, p. 184.
[22] J.H. Sinfelt, in: J.R. Anderson, M. Boudart (Eds.), Catalysis, Science and Technology, Vol. 1, Springler, Berlin, 1981, p. 257.
[23] W.M.H. Sachtler, R.A. van Santen, Adv. Catal. 26 (1983) 69.
[24] S.R. De Miguel, A.O. Scelza, A.A. Castro, Appl. Catal. 44 (1988) 23.
[25] Z. Paál, J. Catal. 105 (1987) 540.
[26] E. Christoffel, F. Fetting, H. Vierrath, J. Catal. 40 (1975) 349.
[27] A. Palazov, Ch. Bonev, D. Shopov, G. Lietz, A. Sárkány, J. Völter, J. Catal. 103 (1987) 249.
[28] J. Sanchez, N. Segovia, A. Moronta, A. Arteaga, G. Arteaga, E. Choren, Appl. Catal. A: Gen. 101 (1993) 199.
[29] H. Verbeek, W.M.H. Sachtler, J. Catal. 42 (1976) 257.
[30] C. Betizeau, G. Leclercq, R. Maurel, C. Bolívar, H. Charcosset, R. Frety, L. Tournayan, J. Catal. 45 (1976) 179.
[31] V.K. Shum, J.B. Butt, W.M.H. Sachtler, J. Catal. 99 (1986) 126.
[32] C.G. Myers, W.H. Lang, P.B. Weisz, Ind. Eng. Chem. 53 (1961) 299.
[33] J.M. Parera, N.S. Fígoli, J.N. Beltramini, E.J. Churin, R.A. Cabrol, in: Proceedings of the 8th International Congress on Catalysis, Verlag Chemie, Berlin, 1984, p. 593.
[34] J. Beltramini, D. Trimm, Appl. Catal. 31 (1987) 113.
[35] F.M. Dautzenberg, J.N. Helle, P. Biloen, W.M.H. Sachtler, J. Catal. 63 (1980) 119.
[36] J.M. Parera, J.N. Beltramini, J. Catal. 112 (1988) 357.
[37] C.R. Apesteguía, T.F. Garetto, C.E. Brema, J.M. Parera, Appl. Catal. 10 (1984) 291.
[38] C.R. Apesteguía, C. Brema, T.F. Garetto, A. Borgna, J.M. Parera, J. Catal. 89 (1984) 52.
[39] C.R. Apesteguía, T.F. Garetto, A. Borgna, J. Catal. 106 (1987) 73.
[40] A. Borgna, T.F. Garetto, A. Monzón, C.R. Apesteguía, J. Catal. 146 (1994) 69.
[41] T.F. Garetto, A. Borgna, C.R. Apesteguía, in: J.W. Hightower, W.N. Delgass, E. Iglesia, A.T. Bell (Eds.), Stud. Surf. Sci. Catal., Vol. 101, Elsevier, Amsterdam, 1996, p. 1155.
[42] C.H. Bartholomew, P. Agrawal, J. Katzer, Adv. Catal. 31 (1982) 135.
[43] C.R. Apesteguía, J. Barbier, J. Catal. 76 (1982) 352.
[44] P. Biloen, J. Helle, H. Verbeek, F. Dautzenberg, W.M.H. Sachtler, J. Catal. 63 (1980) 112.
[45] T.F. Garetto, A. Borgna, C.R. Apesteguía, in: B. Delmon, G.F. Froment (Eds.), Catalyst Deactivation 1994, Elsevier, Amsterdam, 1994, p. 369.
[46] C.L. Pieck, P. Marecot, J. Barbier, Appl. Catal. A: Gen. 145 (1996) 323.
[47] C.A. Querini, N.S. Fígoli, J.M. Parera, Appl. Catal. 53 (1989) 53.